2009

The Impact of QoS Constraints on the Energy Efficiency of Fixed-Rate Wireless Transmissions

Deli Qiao
University of Nebraska-Lincoln, dlqiao@ce.ecnu.edu.cn

M. Cenk Gursoy
University of Nebraska-Lincoln, gursoy@engr.unl.edu

Senem Velipasalar
University of Nebraska-Lincoln, velipasa@engr.unl.edu

The Impact of QoS Constraints on the Energy Efficiency of Fixed-Rate Wireless Transmissions

Deli Qiao, *Student Member, IEEE*, Mustafa Cenk Gursoy, *Member, IEEE*, and Senem Velipasalar, *Member, IEEE*

***Abstract*—Transmission over wireless fading channels under quality of service (QoS) constraints is studied when only the receiver has channel side information. Being unaware of the channel conditions, transmitter is assumed to send the information at a fixed rate. Under these assumptions, a two-state (ON-OFF) transmission model is adopted, where information is transmitted reliably at a fixed rate in the ON state while no reliable transmission occurs in the OFF state. QoS limitations are imposed as constraints on buffer violation probabilities, and effective capacity formulation is used to identify the maximum throughput that a wireless channel can sustain while satisfying statistical QoS constraints. Energy efficiency is investigated by obtaining the bit energy required at zero spectral efficiency and the wideband slope in both wideband and low-power regimes assuming that the receiver has perfect channel side information (CSI). Initially, the wideband regime with multipath sparsity is investigated, and the minimum bit energy and wideband slope expressions are found. It is shown that the minimum bit energy requirements increase as the QoS constraints become more stringent. Subsequently, the low-power regime, which is also equivalent to the wideband regime with rich multipath fading, is analyzed. In this case, bit energy requirements are quantified through the expressions of bit energy required at zero spectral efficiency and wideband slope. It is shown for a certain class of fading distributions that the bit energy required at zero spectral efficiency is indeed the minimum bit energy for reliable communications. Moreover, it is proven that this minimum bit energy is attained in all cases regardless of the strictness of the QoS limitations. The impact upon the energy efficiency of multipath sparsity and richness is quantified, and comparisons with variable-rate/fixed-power and variable-rate/variable-power cases are provided.**

***Index Terms*—Bit energy, effective capacity, energy efficiency, fading channels, fixed-rate transmission, low-power regime, minimum bit energy, QoS constraints, spectral efficiency, wideband regime, wideband slope.**

I. Introduction

THE two key characteristics of wireless communications that most greatly impact system design and performance are 1) the randomly-varying channel conditions and 2) limited energy resources. In wireless systems, the power of the received signal fluctuates randomly over time due to mobility, changing environment, and multipath fading caused by the constructive and destructive superimposition of the multipath signal components [22]. These random changes in the received signal strength lead to variations in the instantaneous data rates that can be supported by the channel. In addition, mobile wireless systems can only be equipped with limited energy resources, and hence energy efficient operation is a crucial requirement in most cases.

To measure and compare the energy efficiencies of different systems and transmission schemes, one can choose as a metric the energy required to reliably send one bit of information. Information-theoretic studies show that energy-per-bit requirement is generally minimized, and hence the energy efficiency is maximized, if the system operates at low signal-to-noise ratio (SNR) levels and hence in the low-power or wideband regimes. Recently, Verdú in [1] has determined the minimum bit energy required for reliable communication over a general class of channels, and studied the spectral efficiency–bit energy tradeoff in the wideband regime while also providing novel tools that are useful for analysis at low SNRs.

In many wireless communication systems, in addition to energy-efficient operation, satisfying certain quality of service (QoS) requirements is of paramount importance in providing acceptable performance and quality. For instance, in voice over IP (VoIP), interactive-video (e.g,. videoconferencing), and streaming-video applications in wireless systems, latency is a key QoS metric and should not exceed certain levels [23]. On the other hand, wireless channels, as described above, are characterized by random changes in the channel, and such volatile conditions present significant challenges in providing QoS guarantees. In most cases, statistical, rather than deterministic, QoS assurances can be given.

In summary, it is vital for an important class of wireless systems to operate efficiently while also satisfying QoS requirements (e.g., latency, buffer violation probability). Information theory provides the ultimate performance limits and identifies the most efficient use of resources. However, information-theoretic studies and Shannon capacity formulation generally do not address delay and quality of service (QoS) constraints [2]. Recently, Wu and Negi in [4] defined the effective capacity as the maximum constant arrival rate that a given time-varying service process can support while providing statistical QoS guarantees. Effective capacity formulation uses the large deviations theory and incorporates the statistical QoS constraints by capturing the rate of decay of the buffer occupancy probability for large queue lengths. Hence, effective capacity can be regarded as the maximum throughput of a system operating under limitations on the buffer violation probability.

Manuscript received December 3, 2008; revised May 1, 2009; accepted August 12, 2009. The associate editor coordinating the review of this paper and approving it for publication was O. Dabeer.

The authors are with the Department of Electrical Engineering, University of Nebraska-Lincoln, Lincoln, NE, 68588 (e-mail: dqiao726@huskers.unl.edu, {gursoy, velipasa}@engr.unl.edu).

This work was supported by the National Science Foundation under Grants CCF – 0546384 (CAREER) and CNS – 0834753. The material in this paper was presented in part at the IEEE International Conference on Communications (ICC), in Dresden, Germany in June 2009.

Digital Object Identifier 10.1109/TWC.2009.12.081600

In the absence of such limitations, effective capacity specializes to the ergodic capacity. At the other extreme in which deterministic, rather than statistical, limitations are imposed, effective capacity specializes to the delay-limited capacity [3]. Hence, in general, effective capacity formulation, by providing us the performance in the presence of soft constraints on the queue length, enables us to fill in the gap between the results obtained using ergodic and delay-limited capacities (see e.g., [14] for further discussion).

The analysis and application of effective capacity in various settings have attracted much interest recently (see e.g., [5]–[14] and references therein). For instance, Tang and Zhang in [7] considered the effective capacity when both the receiver and transmitter know the instantaneous channel gains, and derived the optimal power and rate adaptation technique that maximizes the system throughput under QoS constraints. These results are extended to multichannel communication systems in [8]. Liu *et al.* in [11] considered fixed-rate transmission schemes and analyzed the effective capacity and related resource requirements for Markov wireless channel models. In this work, the continuous-time Gilbert-Elliott channel with ON and OFF states is adopted as the channel model while assuming the fading coefficients as zero-mean Gaussian distributed. A study of cooperative networks operating under QoS constraints is provided in [12]. In [14], we investigated the energy efficiency under QoS constraints by analyzing the normalized effective capacity (or equivalently the spectral efficiency) in the low-power and wideband regimes. We considered variable-rate/variable-power and variable-rate/fixed-power transmission schemes assuming the availability of channel side information at both the transmitter and receiver or only at the receiver.

In this paper, we consider a wireless communication scenario in which only the receiver has the perfect channel side information, and the transmitter, not knowing the channel fading coefficients, sends the information at a fixed-rate with fixed power. If the fixed-rate transmission cannot be supported by the channel, we assume that outage occurs and information has to be retransmitted. This is accomplished by employing a simple automatic repeat request (ARQ) mechanism in which the receiver at the end of each frame duration sends one bit feedback to the transmitter, indicating the success or failure of the transmission. Similarly as in [11], we consider a channel model with ON and OFF states. In this scenario, we investigate the energy efficiency under QoS constraints in the low-power and wideband regimes by considering the bit energy requirement defined as average energy normalized by the effective capacity.

The rest of the paper is organized as follows. Section II introduces the system model. In Section III, we briefly describe the notion of effective capacity and the spectral efficiency–bit energy tradeoff. In Section IV, we analyze the energy efficiency in the wideband regime under the assumption of sparse multipath fading. Energy efficiency in the low-power regime is investigated in Section V. Finally, Section VI provides conclusions while proofs of several theorems are relegated to the Appendix.

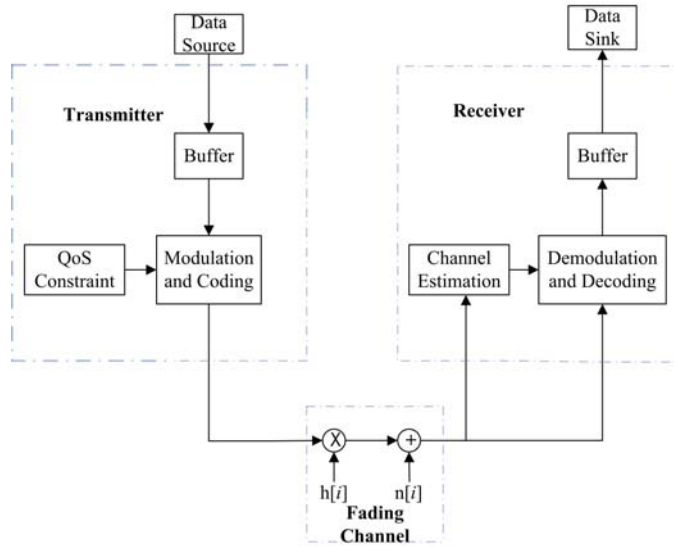

Fig. 1. The general system model.

II. System Model

We consider a point-to-point wireless link in which there is one source and one destination. The system model is depicted in Figure 1. It is assumed that the source generates data sequences which are divided into frames of duration T. These data frames are initially stored in the buffer before they are transmitted over the wireless channel. The discrete-time channel input-output relation in the ith symbol duration is given by

$$y[i] = h[i]x[i] + n[i] \quad i = 1, 2, \ldots. \tag{1}$$

where $x[i]$ and $y[i]$ denote the complex-valued channel input and output, respectively. We assume that the bandwidth available in the system is B and the channel input is subject to the following average energy constraint: $\mathbb{E}\{|x[i]|^2\} \leq \bar{P}/B$ for all i. Since the bandwidth is B, symbol rate is assumed to be B complex symbols per second, indicating that the average power of the system is constrained by $\bar{P}$. Above in (1), $n[i]$ is a zero-mean, circularly symmetric, complex Gaussian random variable with variance $\mathbb{E}\{|n[i]|^2\} = N_0$. The additive Gaussian noise samples $\{n[i]\}$ are assumed to form an independent and identically distributed (i.i.d.) sequence. Finally, $h[i]$ denotes the channel fading coefficient, and $\{h[i]\}$ is a stationary and ergodic discrete-time process. We denote the magnitude-square of the fading coefficients by $z[i] = |h[i]|^2$.

In this paper, we consider the scenario in which the receiver has perfect channel side information and hence perfectly knows the instantaneous values of $\{h[i]\}$ while the transmitter has no such knowledge. In this case, the instantaneous channel capacity with channel gain $z[i]$=$|h[i]|^2$ is

$$C[i] = B\log_2(1 + \text{SNR}z[i]) \text{ bits/s} \tag{2}$$

where $\text{SNR} = \bar{P}/(N_0 B)$ is the average transmitted signal-to-noise ratio. Since the transmitter is unaware of the channel conditions, information is transmitted at a fixed rate of r bits/s. When $r < C$, the channel is considered to be in the ON state and reliable communication is achieved at this

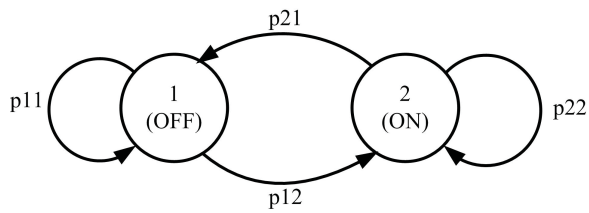

Fig. 2. ON-OFF state transition model.

rate. From information-theoretic arguments, this is possible if strong codes with large blocklength is employed in the system. Since there are TB symbols in each block, we assume TB is large enough to establish reliable communication. If, on the other hand, $r \geq C$, outage occurs. In this case, channel is in the OFF state and reliable communication at the rate of r bits/s cannot be attained. Hence, effective data rate is zero and information has to be resent. We assume that a simple ARQ mechanism is incorporated in the communication protocol to acknowledge the reception of data and to ensure that the erroneous data is retransmitted [11].

Fig. 2 depicts the two-state transmission model together with the transition probabilities. In this paper, we assume that the channel fading coefficients stay constant over the frame duration T. Hence, the state transitions occur at every T seconds. Now, the probability of staying in the ON state, p_{22}, is defined as follows[1]:

$$\begin{aligned} p_{22} &= P\{r < C[i+TB] \,|\, r < C[i]\} \\ &= P\{z[i+TB] > \alpha \,|\, z[i] > \alpha\} \end{aligned} \tag{3}$$

where

$$\alpha = \frac{2^{\frac{r}{B}} - 1}{\text{SNR}}. \tag{4}$$

Note that p_{22} depends on the joint distribution of $(z[i+TB], z[i])$. For the Rayleigh fading channel, the joint density function of the fading amplitudes can be obtained in closed-form [18]. In this paper, with the goal of simplifying the analysis and providing results for arbitrary fading distributions, we assume that fading realizations are independent for each frame[2]. Hence, we basically consider a block-fading channel model. Note that in block-fading channels, the duration T over which the fading coefficients stay constant can be varied to model fast or slow fading scenarios.

Under the block fading assumption, we now have $p_{22} = P\{z[i+TB] > \alpha\} = P\{z > \alpha\}$. Similarly, the other transition probabilities become

$$\begin{aligned} p_{11} = p_{21} &= P\{z \leq \alpha\} = \int_0^{\alpha} p_z(z)dz \quad \text{and} \\ p_{22} = p_{12} &= P\{z > \alpha\} = \int_{\alpha}^{\infty} p_z(z)dz \end{aligned} \tag{5}$$

where p_z is the probability density function of z. Throughout the paper, we assume that both $p_z(z)$ and the cumulative distribution function $P\{z \leq \alpha\}$ are differentiable. We finally note that rT bits are successfully transmitted and received in the ON state, while the effective transmission rate in the OFF state is zero.

III. Preliminaries – Effective Capacity and Spectral Efficiency-Bit Energy Tradeoff

In [4], Wu and Negi defined the effective capacity as the maximum constant arrival rate[3] that a given service process can support in order to guarantee a statistical QoS requirement specified by the QoS exponent θ. If we define Q as the stationary queue length, then θ is the decay rate of the tail of the distribution of the queue length Q:

$$\lim_{q \to \infty} \frac{\log P\{Q \geq q\}}{q} = -\theta. \tag{6}$$

Therefore, for large $q_{\max}$, we have the following approximation for the buffer violation probability: $P\{Q \geq q_{\max}\} \approx e^{-\theta q_{max}}$. Hence, while larger θ corresponds to more strict QoS constraints, smaller θ implies looser QoS guarantees. Moreover, if D denotes the steady-state delay experienced in the buffer, then it is shown in [13] that $P\{D \geq d_{\max}\} \leq c\sqrt{P\{Q \geq q_{\max}\}}$ for constant arrival rates. This result provides a link between the buffer and delay violation probabilities. In the above formulation, c is some positive constant, $q_{\max} = ad_{\max}$, and a is the source arrival rate. Therefore, effective capacity provides the maximum arrival rate when the system is subject to statistical queue length or delay constraints in the forms of $P\{Q \geq q_{\max}\} \leq e^{-\theta q_{max}}$ or $P\{D \geq d_{\max}\} \leq c\, e^{-\theta a\, d_{max}/2}$, respectively. Since the average arrival rate is equal to the average departure rate when the queue is in steady-state [17], effective capacity can also be seen as the maximum throughput in the presence of such constraints. We also note that effective capacity characterizes the performance in the large-queue-length regime. If the queue length is finite and small, supported arrival rates will be smaller than predicted by the effective capacity. Additionally, in such cases, packet and data loss events, occurring when the queue is full, should also be explicitly considered. Hence, systems with limited queue length require in general more energy, and results presented in this paper in the large-queue-length regime can be regarded as fundamental limits that can be used as benchmarks for such systems.

The effective capacity for a given QoS exponent θ is obtained from

$$-\lim_{t \to \infty} \frac{1}{\theta t} \log_e \mathbb{E}\{e^{-\theta S[t]}\} \stackrel{\text{def}}{=} -\frac{\Lambda(-\theta)}{\theta} \tag{7}$$

where $S[t] = \sum_{k=1}^{t} R[k]$ is the time-accumulated service process and $\{R[k], k = 1, 2, \ldots\}$ denote the discrete-time, stationary and ergodic stochastic service process. Note that in the model we consider, $R[k] = rT$ or 0 depending on the channel state being ON or OFF, respectively. In [15] and [16, Section 7.2, Example 7.2.7], it is shown that for such an ON-OFF model, $\frac{\Lambda(\theta)}{\theta}$ is given by (8) on the next page.

Using the formulation in (8) and noting that $p_{11} + p_{22} = 1$ in our model, we express the effective capacity normalized by the

[1]The formulation in (3) assumes as before that the symbol rate is B symbols/s and hence we have TB symbols in a duration of T seconds.

[2]This assumption also enables us to compare the results of this paper with those in [14] in which variable-rate/variable-power and variable-rate/fixed-power transmission schemes are studied for block fading channels.

[3]For time-varying arrival rates, effective capacity specifies the effective bandwidth of the arrival process that can be supported by the channel.

$$\frac{\Lambda(\theta)}{\theta} = \frac{1}{\theta}\log_e\left(\frac{1}{2}\left(p_{11} + p_{22}e^{\theta T r} + \sqrt{(p_{11} + p_{22}e^{\theta T r})^2 + 4(p_{11} + p_{22} - 1)e^{\theta T r}}\right)\right). \tag{8}$$

frame duration T and bandwidth B, or equivalently spectral efficiency in bits/s/Hz, for a given statistical QoS constraint θ, as

$$\begin{aligned}
&\mathsf{R}_E(\text{SNR}, \theta) \\
&= \frac{1}{TB}\max_{r\geq 0}\left\{-\frac{\Lambda(-\theta)}{\theta}\right\} && (9)\\
&= \max_{r\geq 0}\left\{-\frac{1}{\theta TB}\log_e\left(p_{11} + p_{22}e^{-\theta T r}\right)\right\} && (10)\\
&= \max_{r\geq 0}\left\{-\frac{1}{\theta TB}\log_e\left(1 - P\{z > \alpha\}(1 - e^{-\theta T r})\right)\right\} && (11)\\
&= -\frac{1}{\theta TB}\log_e\left(1 - P\{z > \alpha_{\text{opt}}\}\left(1 - e^{-\theta T r_{\text{opt}}}\right)\right) \text{ bits/s/Hz} && (12)
\end{aligned}$$

where r_{opt} is the maximum fixed transmission rate that solves (11) and $\alpha_{\text{opt}} = (2^{\frac{r_{\text{opt}}}{B}} - 1)/\text{SNR}$. Note that both α_{opt} and r_{opt} are functions of SNR and θ.

The normalized effective capacity, R_E, provides the maximum throughput under statistical QoS constraints in the fixed-rate transmission model. It can be easily shown that

$$\lim_{\theta\to 0}\mathsf{R}_E(\text{SNR}, \theta) = \max_{r\geq 0}\ \frac{r}{B}P\{z > \alpha\}. \tag{13}$$

Hence, as the QoS requirements relax, the maximum constant arrival rate approaches the average transmission rate. On the other hand, for $\theta > 0$, $\mathsf{R}_E < \frac{1}{B}\max_{r\geq 0} rP\{z > \alpha\}$ in order to avoid violations of QoS constraints.

In this paper, we focus on the energy efficiency of wireless transmissions under the aforementioned statistical QoS limitations. Since energy efficient operation generally requires operation at low-SNR levels, our analysis throughout the paper is carried out in the low-SNR regime. In this regime, the tradeoff between the normalized effective capacity (i.e, spectral efficiency) R_E and bit energy $\frac{E_b}{N_0} = \frac{\text{SNR}}{\mathsf{R}_E(\text{SNR})}$ is a key tradeoff in understanding the energy efficiency, and is characterized by the bit energy at zero spectral efficiency and wideband slope provided, respectively, by

$$\begin{aligned}
\left.\frac{E_b}{N_0}\right|_{\mathsf{R}_E=0} &= \lim_{\text{SNR}\to 0}\frac{\text{SNR}}{\mathsf{R}_E(\text{SNR})} = \frac{1}{\dot{\mathsf{R}}_E(0)}, \quad \text{and}\\
\mathcal{S}_0 &= -\frac{2(\dot{\mathsf{R}}_E(0))^2}{\ddot{\mathsf{R}}_E(0)}\log_e 2
\end{aligned} \tag{14}$$

where $\dot{\mathsf{R}}_E(0)$ and $\ddot{\mathsf{R}}_E(0)$ are the first and second derivatives with respect to SNR, respectively, of the function $\mathsf{R}_E(\text{SNR})$ at zero SNR [1]. $\left.\frac{E_b}{N_0}\right|_{\mathsf{R}_E=0}$ and $\mathcal{S}_0$ provide a linear approximation of the spectral efficiency curve at low spectral efficiencies, i.e.,

$$\mathsf{R}_E\left(\frac{E_b}{N_0}\right) = \frac{\mathcal{S}_0}{10\log_{10}2}\left(\left.\frac{E_b}{N_0}\right|_{dB} - \left.\frac{E_b}{N_0}\right|_{\mathsf{R}_E=0,dB}\right) + \epsilon \tag{15}$$

where $\epsilon = o\left(\frac{E_b}{N_0} - \left.\frac{E_b}{N_0}\right|_{\mathsf{R}_E=0}\right)$.

Above, $\left.\frac{E_b}{N_0}\right|_{dB} = 10\log_{10}\frac{E_b}{N_0}$. When the spectral efficiency R_E is a non-decreasing concave function of SNR, the bit energy $\frac{E_b}{N_0}$ diminishes with decreasing spectral efficiency. Hence, in this case, the bit energy required at zero spectral efficiency is indeed the minimum one, i.e., $\left.\frac{E_b}{N_0}\right|_{\mathsf{R}_E=0} = \frac{E_b}{N_0}_{\min}$.

IV. Energy Efficiency in the Wideband Regime – Sparse Multipath Fading Case

In this section, we consider the wideband regime in which the bandwidth is large. We assume that the average power $\bar{P}$ is kept constant. Note that as the bandwidth B increases, $\text{SNR} = \frac{\bar{P}}{N_0 B}$ approaches zero and we operate in the low-SNR regime.

Following the approach generally employed in information-theoretic analyses, we assume that the wideband channel is decomposed into N parallel subchannels. We further assume that each subchannel has a bandwidth that is equal to the coherence bandwidth, B_c. Therefore, independent flat-fading is experienced in each subchannel, and we have $B = NB_c$. Similar to (1), the input-output relation in the kth subchannel can be written as

$$y_k[i] = h_k[i]x_k[i] + n_k[i] \quad i = 1, 2, \ldots \text{ and } k = 1, 2, \ldots, N. \tag{16}$$

The fading coefficients $\{h_k\}_{k=1}^n$ in different subchannels are assumed to be independent. The signal-to-noise ratio in the kth subchannel is $\text{SNR}_k = \frac{\bar{P}_k}{N_0 B_c}$ where $\bar{P}_k$ denotes the power allocated to the kth subchannel and we have $\sum_{k=1}^N \bar{P}_k = \bar{P}$. Over each subchannel, the same transmission strategy as described in Section II is employed. Therefore, the transmitter, not knowing the fading coefficients of the subchannels, sends the data over each subchannel at the fixed rate of r. If $r < B_c\log(1 + \text{SNR}_k z_k[i])$ where $z_k = |h_k|^2$, then transmission over the kth subchannel is successful. Otherwise, retransmission is required. Hence, we have an ON-OFF state model for each subchannel. On the other hand, for the transmission over N subchannels, we have a state-transition model with $N+1$ states because we have overall the following $N+1$ possible total transmission rates: $\{0, rT, 2rT, \ldots, NrT\}$. For instance, if all N subchannels are in the OFF state simultaneously, the total rate is zero. If j out of N subchannels are in the ON state, then the rate is jrT.

Now, assume that the states are enumerated in the increasing order of the total transmission rates supported by them. Hence, in state $j \in \{1, \ldots, N+1\}$, the transmission rate is $(j-1)rT$. The transition probability from state $i \in \{1, \ldots, N+1\}$ to state $j \in \{1, \ldots, N+1\}$ is given by (17) on the next page where $\mathcal{I}_{j-1}$ denotes a subset of the index set $\{1, \ldots, N\}$ with $j-1$ elements. The summation in (17) is over all such subsets. Moreover, in (17), $\mathcal{I}_{j-1}^c$ denotes the complement of the set $\mathcal{I}_{j-1}$, and $\alpha_k = \frac{2^{\frac{r}{B_c}}-1}{\text{SNR}_k}$. Note in the above formulation that the transition probabilities, p_{ij}, do not depend on the initial state i due to the block-fading assumption. If, in addition to

$$p_{ij} = p_j = P\{(j-1) \text{ subchannels out of } N \text{ subchannels are in the ON state}\}$$
$$= \sum_{\mathcal{I}_{j-1} \subset \{1,\ldots,N\}} \left(\prod_{k \in \mathcal{I}_{j-1}} P\{z_k > \alpha_k\} \prod_{k \in \mathcal{I}_{j-1}^c} (1 - P\{z_k > \alpha_k\}) \right) \tag{17}$$

being independent, the fading coefficients and hence $\{z_k\}_{k=1}^N$ in different subchannels are identically distributed, then p_{ij} in (17) simplifies and becomes a binomial probability:

$$p_{ij} = p_j = \binom{N}{j-1} (P\{z > \alpha\})^{j-1} (1 - P\{z > \alpha\})^{N-j+1}. \tag{18}$$

Note that if the fading coefficients are i.i.d., the total power should be uniformly distributed over the subchannels. Hence, in this case, we have $\bar{P}_k = \frac{\bar{P}}{N}$ and therefore $\text{SNR}_k = \frac{\bar{P}_k}{N_0 B_c} = \frac{\bar{P}/N}{N_0 B/N} = \frac{\bar{P}}{N_0 B} = \text{SNR}$ which is equal to the original SNR definition used in (2). Now, we have the same $\alpha = \frac{2^{\frac{r}{B_c}}-1}{\text{SNR}}$ for each subchannel.

The effective capacity of this wideband channel model is given by the following result.

Theorem 1: For the wideband channel with N parallel noninteracting subchannels each with bandwidth B_c and independent flat fading, the normalized effective capacity in bits/s/Hz is

$$\mathsf{R}_E(\text{SNR}, \theta) = \max_{\substack{r \geq 0 \\ \bar{P}_k \geq 0 \text{ s.t. } \sum \bar{P}_k \leq \bar{P}}} \left\{ -\frac{1}{\theta T B} \log_e \left(\sum_{j=1}^{N+1} p_j \, e^{-\theta(j-1)rT} \right) \right\} \tag{19}$$

where p_j is given in (17). If $\{z_k\}_{k=1}^N$ are identically distributed, then the normalized effective capacity expression simplifies to

$$\mathsf{R}_E(\text{SNR}, \theta) = \max_{r \geq 0} \left\{ -\frac{1}{\theta T B_c} \log_e \left(1 - P\{z > \alpha\}(1 - e^{-\theta T r})\right) \right\}. \tag{20}$$

where $\alpha = \frac{2^{\frac{r}{B_c}}-1}{\text{SNR}}$ and $\text{SNR} = \frac{\bar{P}}{N_0 B}$.

Proof: See Appendix A.

Theorem 1 shows that the effective capacity of a wideband channel with N subchannels each with i.i.d. flat fading has an expression similar to that in (11), which provides the effective capacity of a single channel experiencing flat fading. The only difference between (11) and (20) is that B is replaced in (20) by B_c, which is the bandwidth of each subchannel.

In this section, we consider the wideband regime in which the overall bandwidth of the system, B, is large. In particular, we analyze the performance in the scenario of sparse multipath fading. Motivated by the recent measurement studies in the ultrawideband regime, the authors in [19] and [20] considered sparse multipath fading channels and analyzed the performance under channel uncertainty, employing the Shannon capacity formulation as the performance metric. In particular, [19] and [20] noted that the number of independent resolvable paths in sparse multipath channels increase at most sublinearly with the bandwidth, which in turn causes the coherence bandwidth B_c to increase with increasing bandwidth. To characterize the performance of sparse fading channels in the wideband regime, we assume in this section that $B_c \to \infty$ as $B \to \infty$. We further assume that the the number of subchannels N remains bounded and hence the degrees of freedom are limited. For instance, this case arises if the number of resolvable paths are bounded even at infinite bandwidth. Such a scenario is considered in [21] where the capacity and mutual information are characterized under channel uncertainty in the wideband regime with bounded number of paths.

The case of rich multipath fading in which B_c remains fixed and N grows without bound and the scenario in which both B_c and N increase to infinity are treated in Section V because each subchannel in these cases operates in the low-power regime as N increases.

We first introduce the notation $\zeta = \frac{1}{B_c}$. Note that as $B_c \to \infty$, we have $\zeta \to 0$. Moreover, with this notation, the normalized effective capacity in (20) given for i.i.d. fading can, after maximization, be expressed as[4]

$$\mathsf{R}_E(\text{SNR}) = -\frac{\zeta}{\theta T} \log_e \left(1 - P\{z > \alpha_{\text{opt}}\}\left(1 - e^{-\theta T r_{\text{opt}}}\right)\right). \tag{21}$$

Note that α_{opt} and r_{opt} are also in general dependent on B_c and hence ζ. The following result provides the expressions for the minimum bit energy, which is achieved at zero spectral efficiency (i.e., as $B \to \infty$ and $B_c \to \infty$), and the wideband slope, and characterizes the spectral efficiency-bit energy tradeoff in the wideband regime when multipath fading is sparse, the number of subchannels is bounded, and the fading coefficients are i.i.d. in different subchannels.

Theorem 2: In sparse multipath fading wideband channels with bounded number of subchannels each with i.i.d. fading coefficients, the minimum bit energy and wideband slope are given by

$$\frac{E_b}{N_0}_{\min} = \frac{-\delta \log_e 2}{\log_e \xi} \quad \text{and} \tag{22}$$

$$\mathcal{S}_0 = \frac{2\xi \log_e^2 \xi}{(\delta \alpha_{\text{opt}}^*)^2 P\{z > \alpha_{\text{opt}}^*\} e^{-\delta \alpha_{\text{opt}}^*}}, \tag{23}$$

respectively, where $\delta = \frac{\theta T \bar{P}}{N N_0 \log_e 2}$ and $\xi = 1 - P\{z > \alpha_{\text{opt}}^*\}(1 - e^{-\delta \alpha_{\text{opt}}^*})$. α_{opt}^* is defined as $\alpha_{\text{opt}}^* = \lim_{\zeta \to 0} \alpha_{\text{opt}}$ and

[4]Since the results in the paper are generally obtained for fixed but arbitrary θ, the normalized effective capacity is often expressed in the paper as $\mathsf{R}_E(\text{SNR})$ instead of $\mathsf{R}_E(\text{SNR}, \theta)$ to avoid cumbersome expressions.

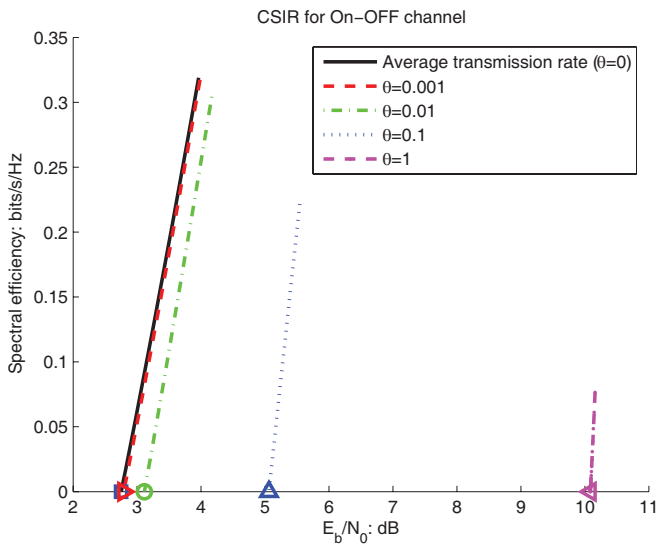

Fig. 3. Spectral efficiency vs. E_b/N_0 in the Rayleigh channel.

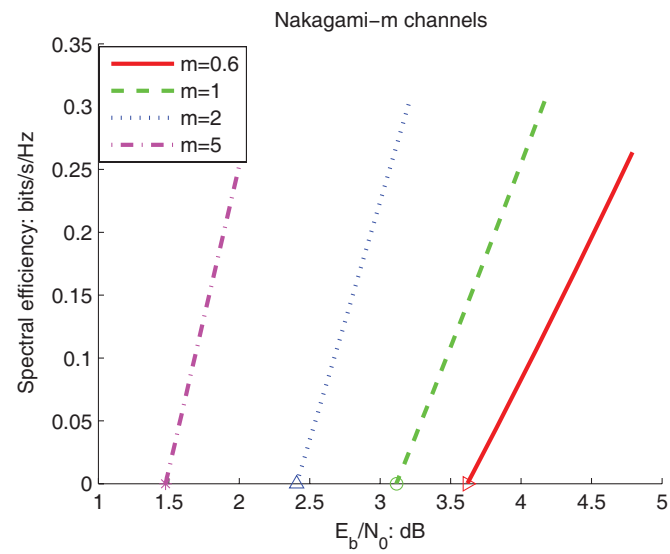

Fig. 4. Spectral efficiency vs. E_b/N_0 in Nakagami-m channels; $\theta = 0.01$, $m = 0.6, 1, 2, 5$.

α^*_{opt} satisfies

$$\delta\alpha^*_{\text{opt}} = \log_e\left(1 + \delta\frac{P\{z > \alpha^*_{\text{opt}}\}}{p_z(\alpha^*_{\text{opt}})}\right). \tag{24}$$

Proof: See Appendix B.

Remark: Theorem 2, through the minimum bit energy and wideband slope expressions, quantifies the bit energy requirements in the wideband regime when the system is operating subject to statistical QoS constraints specified by θ. Note that both $\frac{E_b}{N_0}_{\min}$ and $\mathcal{S}_0$ depend on the QoS exponent θ through δ. As will be observed in the numerical results, $\frac{E_b}{N_0}_{\min}$ and the bit energy requirements at nonzero spectral efficiency values generally increase with increasing θ. Moreover, when compared with the results in Section V, it will be seen that sparse multipath fading and having a bounded number of subchannels incur energy penalty in the presence of QoS constraints while performances do not depend on the multipath sparsity when there are no such constraints and hence $\theta = 0$.

Having analytically characterized the spectral efficiency–bit energy tradeoff in the wideband regime in Theorem 2, we now provide numerical results to illustrate the theoretical findings. Fig. 3 plots the spectral efficiency curves as a function of the bit energy in the Rayleigh channel. In all the curves, we have $\bar{P}/(NN_0) = 10^4$. Moreover, we set $T = 2$ ms in the numerical results throughout the paper. As predicted by the result of Theorem 2, $\left.\frac{E_b}{N_0}\right|_{\mathsf{R}_E=0} = \frac{E_b}{N_0}_{\min}$ in all cases in Fig. 3. It can be found that $\alpha^*_{\text{opt}} = \{1, 0.9858, 0.8786, 0.4704, 0.1177\}$ from which we obtain $\frac{E_b}{N_0}_{\min} = \{2.75, 2.79, 3.114, 5.061, 10.087\}$dB for $\theta = \{0, 0.001, 0.01, 0.1, 1\}$, respectively. For the same set of θ values in the same sequence, we compute the wideband slope values as $\mathcal{S}_0 = \{0.7358, 0.7463, 0.8345, 1.4073, 3.1509\}$. We immediately observe that more stringent QoS constraints and hence higher values of θ lead to higher minimum bit energy values and also higher energy requirements at other nonzero spectral efficiencies. Fig. 4 provides the spectral efficiency curves for Nakagami-m fading channels for different values of m. In this figure, we set $\theta = 0.01$. For $m = 0.6, 1, 2, 5$, we find that $\alpha^*_{\text{opt}} = \{1.0567, 0.8786, 0.7476, 0.6974\}$, $\frac{E_b}{N_0}_{\min} = \{3.618, 3.114, 2.407, 1.477\}$, and $\mathcal{S}_0 = \{0.6382, 0.8345, 1.1220, 1.4583\}$, respectively. Note that as m increases and hence the channel conditions improve, the minimum bit energy decreases and the wideband slope increases, improving the energy efficiency both at zero spectral efficiency and at nonzero but small spectral efficiency values. As $m \to \infty$, the performance approaches that of the unfaded additive Gaussian noise channel (AWGN) for which we have $\frac{E_b}{N_0}_{\min} = -1.59$ dB and $\mathcal{S}_0 = 2$ [1].

V. Energy Efficiency in the Low-Power Regime

In this section, we investigate the spectral efficiency–bit energy tradeoff in a single flat-fading channel as the average power $\bar{P}$ diminishes. We assume that the bandwidth allocated to the channel is fixed. Note that $\text{SNR} = \bar{P}/(N_0B)$ vanishes with decreasing $\bar{P}$, and we again operate in the low-SNR regime similarly as in Section IV. Note further from (12) that the effective capacity of a flat-fading channel is given by

$$\mathsf{R}_E(\text{SNR}) = -\frac{1}{\theta TB}\log_e\left(1 - P\{z > \alpha_{\text{opt}}\}\left(1 - e^{-\theta T r_{\text{opt}}}\right)\right). \tag{25}$$

On the other hand, we remark that the results derived here also apply to the wideband regime under the assumption that the number of non-interacting subchannels increases without bound with increasing bandwidth. Note that in such a case, each subchannel operates in the low-power regime.

The following result provides the expressions for the bit energy at zero spectral efficiency and the wideband slope.

Theorem 3: In the low-power regime, the bit energy at zero spectral efficiency and wideband slope are given by

$$\left.\frac{E_b}{N_0}\right|_{\mathrm{R}_E=0} = \frac{\log_e 2}{\alpha^*_{\text{opt}} P\{z > \alpha^*_{\text{opt}}\}} \quad \text{and} \tag{26}$$

$$\mathcal{S}_0 = \frac{2P\{z > \alpha^*_{\text{opt}}\}}{1+\beta(1-P\{z > \alpha^*_{\text{opt}}\})}, \tag{27}$$

respectively, where $\beta = \frac{\theta T B}{\log_e 2}$ is the normalized QoS constraint. In the above formulation, α^*_{opt} is defined as $\alpha^*_{\text{opt}} = \lim_{\text{SNR}\to 0} \alpha_{\text{opt}}$, and α^*_{opt} satisfies

$$\alpha^*_{\text{opt}} p_z(\alpha^*_{\text{opt}}) = P\{z > \alpha^*_{\text{opt}}\}. \tag{28}$$

Proof: See Appendix C.

Corollary 1: The same bit energy and wideband slope expressions as in (26) and (27) are achieved in the wideband regime as $B \to \infty$ if the fading coefficients in different subchannels are i.i.d. and also if the number of subchannels N increases linearly with increasing bandwidth (as in rich multipath fading channels), keeping the coherence bandwidth fixed.

Under the assumptions stated in Corollary 1, the effective capacity is given by (20). Moreover, as $B \to \infty$, we have B_c fixed while $N \to \infty$. Hence, $\text{SNR} = \frac{\bar{P}/N}{N_0 B_c} \to 0$. This setting is exactly the same as the low-power regime considered in Theorem 3. Therefore, the results of Theorem 3 apply immediately.

Next, we show that equation (28) that needs to be satisfied by α^*_{opt} has a unique solution for a certain class of fading distributions.

Theorem 4: Assume that the probability density function of z, denoted by $p_z(\cdot)$, is differentiable, and both $p_z(\cdot)$ and its derivative $\dot{p}_z(\cdot)$ at the origin do not contain impulses or higher-order singularities and are finite. Assume further that the support of $p_z(\cdot)$ is $[0,\infty)$. Under these assumptions, if $2p_z(x)+x\dot{p}_z(x) = 0$ is solved at a single point $x_0 > 0$ among all $x \in (0,\infty)$, then the equation $\alpha^*_{\text{opt}} p_z(\alpha^*_{\text{opt}}) = P\{z > \alpha^*_{\text{opt}}\}$ has a unique solution.

Proof: We first define $f(x) = xp_z(x) - P\{z > x\}$ for $x \geq 0$.Under the conditions stated in Theorem 4, we can easily see that $f(0) = -1$ and $f(\infty) = 0$. Moreover, $f(x) \geq -1$ for all $x \geq 0$ because $p_z(x) \geq 0$ and $P\{z > x\} \leq 1$. It can also be seen that $\int_0^\infty f(x)dx = \int_0^\infty xp_z(x)dx - \int_0^\infty P\{z > x\}dx = E\{z\} - E\{z\} = 0$. Therefore, there exists $x > 0$ such that $f(x) > 0$.

Differentiating $f(x)$ with respect to x gives $\dot{f}(x) = 2p_z(x) + x\dot{p}_z(x)$. Note that $\dot{f}(0) = 2p_z(0) \geq 0$. Since $f(x) \geq -1$ and $f(0) = -1$, f is necessarily an increasing function initially. Hence, $\dot{f}(x) > 0$ for all $x \in (0, x_0)$ where x_0 is the point at which $f(x_0) = 0$. Since x_0 is the only positive point for which the derivative is zero, and $f(x) > 0$ for some x as discussed above and $f(x)$ has to approach zero as $x \to \infty$, we conclude that $f(x)$ is a decreasing function for all $x > x_0$, and hence $\dot{f}(x) < 0$ for all $x > x_0$. Otherwise, if $\dot{f}(x) > 0$ for some x, $\dot{f}(x)$ never becomes zero again, and $f(x)$ increases indefinitely. Furthermore, we can see that $f(x) > 0$ for all $x \geq x_0$ because if $f(x) < 0$ for some $x \geq x_0$, $f(x)$ should start increasing to zero as $x \to \infty$. However, this is not possible because $\dot{f}(x) < 0$ for all $x > x_0$.

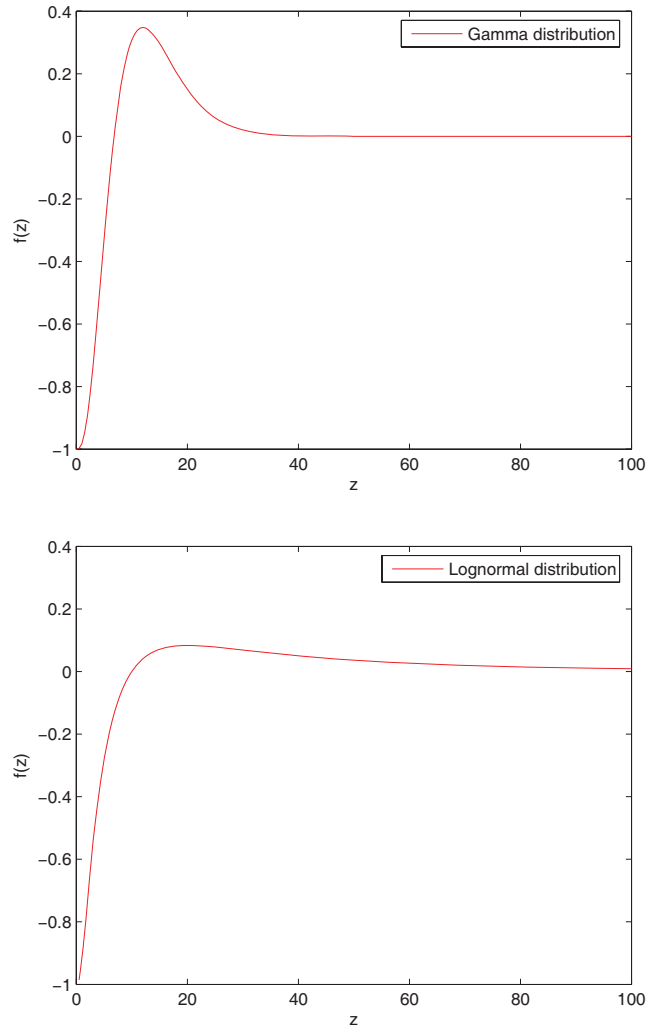

Fig. 5. The plots of the function $f(z)$ for Gamma distribution $p_z(z) = \frac{z^{\alpha-1}e^{-\frac{z}{\beta}}}{\beta^\alpha \Gamma(\alpha)}$ with $\alpha = \beta = 3$, and Lognormal distribution $p_z(z) = \frac{1}{\sigma x\sqrt{2\pi}} e^{-\frac{(\log_e x - m)^2}{2\sigma^2}}$ with $\sigma = 1, m = 2$.

Therefore, we have concluded that $f(0) = -1$ and $f(x)$ is an increasing function in the range $x \in (0, x_0)$. Moreover, $f(x_0) > 0$ and $f(x)$ decreases to zero without being negative as $x \to \infty$. From this, we conclude that $f(x)$ intersects the horizontal axis only once at an x value in between 0 and x_0. Therefore, $f(x) = 0$ has a unique solution. □

Remark: The conditions of Theorem 4 are satisfied by a general class of distributions, including the Gamma distribution,

$$p_z(z) = \frac{z^{\alpha-1}e^{-\frac{z}{\beta}}}{\beta^\alpha \Gamma(\alpha)},$$

where $z, \alpha, \beta > 0$, and Lognormal distribution,

$$p_z(z) = \frac{1}{\sigma z\sqrt{2\pi}} e^{-\frac{(\log_e z - m)^2}{2\sigma^2}},$$

where $z > 0$, $-\infty < m < \infty$, and $\sigma > 0$. Note that in Nakagami-m and Rayleigh fading channels, the distribution of $z = |h|^2$ can be seen as special cases of the Gamma distribution. In Fig. 5, where the function $f(\cdot)$ is plotted for Gamma and Lognormal distributions, we indeed observe that

these distributions satisfy the conditions of Theorem 4 and the function $f(\cdot)$ is equal to zero at a unique point.

Remark: Theorem 3 shows that the $\left.\frac{E_b}{N_0}\right|_{\mathsf{R}_E=0}$ for any $\theta \geq 0$ depends only on α^*_{opt}. From Theorem 4, we know under certain conditions that α^*_{opt} is unique and hence is the same for all $\theta \geq 0$. We immediately conclude from these results that $\left.\frac{E_b}{N_0}\right|_{\mathsf{R}_E=0}$ also has the same value for all $\theta \geq 0$ and therefore does not depend on θ for the class of distributions and channels given in the above Remark.

Moreover, using the results of Theorem 4 above and Theorem 2 in Section IV, we can further show that $\left.\frac{E_b}{N_0}\right|_{\mathsf{R}_E=0}$ is the minimum bit energy. Note that this implies that the same minimum bit energy can be attained regardless of how strict the QoS constraint is. On the other hand, we note that the wideband slope $\mathcal{S}_0$ in general varies with θ.

Corollary 2: In the low-power regime, when $\theta = 0$, the minimum bit energy is achieved as $\bar{P} \to 0$, i.e., $\left.\frac{E_b}{N_0}\right|_{\mathsf{R}_E=0} = \frac{E_b}{N_0}_{\min}$. Moreover, if the probability density function of z satisfies the conditions stated in Theorem 4, then the minimum bit energy is achieved as $\bar{P} \to 0$, i.e. $\left.\frac{E_b}{N_0}\right|_{\mathsf{R}_E=0} = \frac{E_b}{N_0}_{\min}$, for all $\theta \geq 0$.

Proof: Recall from (13) that in the limit as $\theta \to 0$,

$$\mathsf{R}_E(\text{SNR}, 0) = \lim_{\theta \to 0} \mathsf{R}_E(\text{SNR}, \theta) = \max_{r \geq 0} \frac{r}{B} P\left\{z > \frac{2^{\frac{r}{B}} - 1}{\text{SNR}}\right\}. \tag{29}$$

Since the optimization is performed over all $r \geq 0$, it can be easily seen that the above maximization problem can be recast as follows:

$$\mathsf{R}_E(\text{SNR}, 0) = \max_{x \geq 0} x P\left\{z > \frac{2^x - 1}{\text{SNR}}\right\}. \tag{30}$$

From (30), we note that $\mathsf{R}_E(\text{SNR}, 0)$ depends on B only through $\text{SNR} = \frac{\bar{P}}{N_0 B}$. Therefore, increasing B has the same effect as decreasing $\bar{P}$. Hence, low-power and wideband regimes are equivalent when $\theta = 0$. Consequently, the result of Theorem 2, which shows that the minimum bit energy is achieved as $B \to \infty$, implies that the minimum bit energy is also achieved as $\bar{P} \to 0$.

Note that $\mathsf{R}_E(\text{SNR}, \theta) \leq \mathsf{R}_E(\text{SNR}, 0)$ for $\theta > 0$. Therefore, the bit energy required when $\theta > 0$ is larger than that required when $\theta = 0$. On the other hand, as we have proven in Theorem 4, α^*_{opt} is unique and the bit energy required as $\bar{P} \to 0$ is the same for all $\theta \geq 0$ when p_z satisfies certain conditions. Since the minimum bit energy in the case of $\theta = 0$ is achieved as $\bar{P} \to 0$, and the same bit energy is attained for all $\theta > 0$, we immediately conclude that $\left.\frac{E_b}{N_0}\right|_{\mathsf{R}_E=0} = \frac{E_b}{N_0}_{\min}$ for all $\theta \geq 0$ □

Next, we provide numerical results which confirm the theoretical conclusions and illustrate the impact of QoS constraints on the energy efficiency. We set $B = 10^5$ Hz in the computations. Fig. 6 plots the spectral efficiency as a function of the bit energy for different values of θ in the Rayleigh fading channel (or equivalently Nakagami-m fading channel with $m = 1$) for which $\mathbb{E}\{|h|^2\} = \mathbb{E}\{z\} = 1$. In all cases in Fig. 6, we readily note that $\left.\frac{E_b}{N_0}\right|_{\mathsf{R}_E=0} = \frac{E_b}{N_0}_{\min}$. Moreover, as

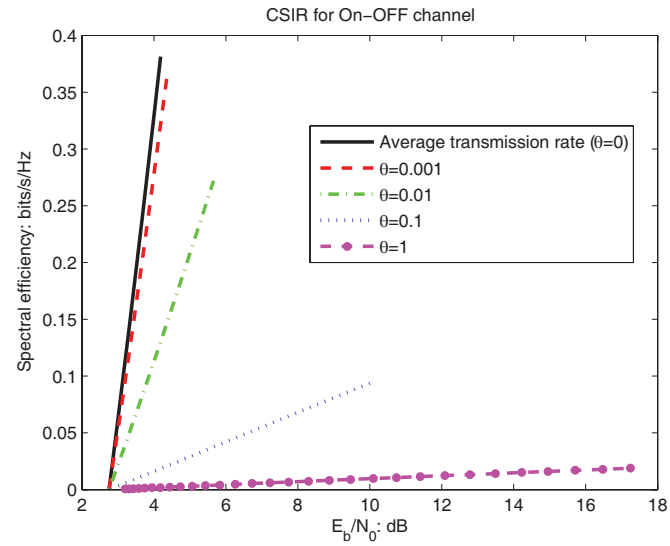

Fig. 6. Spectral efficiency vs. E_b/N_0 in the Rayleigh channel (equivalently Nakagami-m channel with $m = 1$).

predicted, the minimum bit energy is the same and is equal to the one achieved when there are no QoS constraints (i.e., when $\theta = 0$). From the equation $\alpha^*_{\text{opt}} p_z(\alpha^*_{\text{opt}}) = P\{z > \alpha^*_{\text{opt}}\}$, we can find that $\alpha^*_{\text{opt}} = 1$ in the Rayleigh channel for which $p_z(\alpha^*_{\text{opt}}) = P\{z > \alpha^*_{\text{opt}}\} = e^{-\alpha^*_{\text{opt}}}$. Hence, the minimum bit energy is $\frac{E_b}{N_0}_{\min} = 2.75$ dB. On the other hand, the wideband slopes are $\mathcal{S}_0 = \{0.7358, 0.6223, 0.2605, 0.0382, 0.0040\}$ for $\theta = \{0, 0.001, 0.01, 0.1, 1\}$, respectively. Hence, $\mathcal{S}_0$ decreases with increasing θ and consequently more bit energy is required at a fixed nonzero spectral efficiency. Assuming that the minimum bit energies are the same and considering the linear approximation in (15), we can easily show for fixed spectral efficiency $\mathsf{R}_E\left(\frac{E_b}{N_0}\right)$ for which the linear approximation is accurate that the increase in the bit energy in dB, when the QoS exponent increases from θ_1 to θ_2, is

$$\left.\frac{E_b}{N_0}\right|_{dB,\theta_2} - \left.\frac{E_b}{N_0}\right|_{dB,\theta_1} = \left(\frac{1}{\mathcal{S}_{0,\theta_2}} - \frac{1}{\mathcal{S}_{0,\theta_1}}\right) \mathsf{R}_E\left(\frac{E_b}{N_0}\right) 10 \log_{10} 2. \tag{31}$$

As observed in Fig. 6 (and also as will be seen in Fig. 7), spectral efficiency curves are almost linear in the low-power regime, validating the accuracy of the linear approximation in (15) obtained through $\left.\frac{E_b}{N_0}\right|_{\mathsf{R}_E=0}$ and $\mathcal{S}_0$.

Fig. 7 plots the spectral efficiency curves as a function of the bit energy for Nakagami-m channels for different values of m. θ is set to be 0.01. For $m = \{0.6, 1, 2, 5\}$, we compute that $\alpha^*_{\text{opt}} = \{1.2764, 1, 0.809, 0.7279\}$, $\frac{E_b}{N_0}_{\min} = \{3.099, 2.751, 2.176, 1.343\}$, and $\mathcal{S}_0 = \{0.1707, 0.2605, 0.4349, 0.7479\}$, respectively. We observe that as m increases and hence the channel quality improves, lower bit energies are required. Finally, in Fig. 8, we plot the spectral efficiency vs. E_b/N_0 for different transmission strategies. The variable-rate/variable-power and variable-rate/fixed-power strategies are studied in [14]. We immediately see that substantially more energy is required

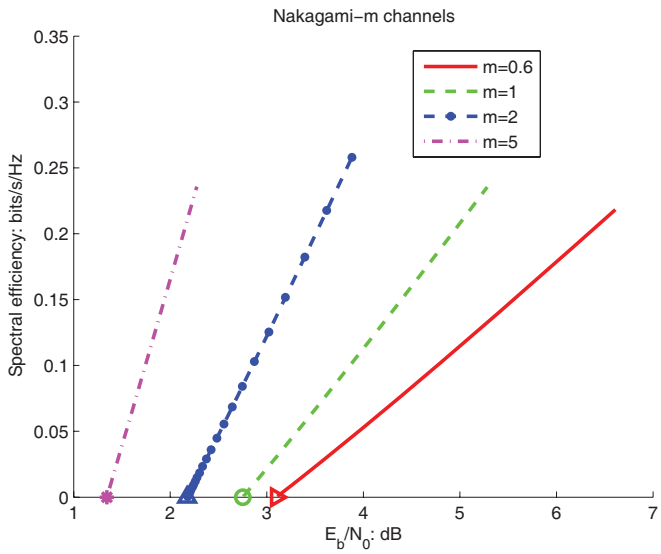

Fig. 7. Spectral efficiency vs. E_b/N_0 in Nakagami-m channels; $\theta = 0.01$, $m = 0.6, 1, 2, 5$.

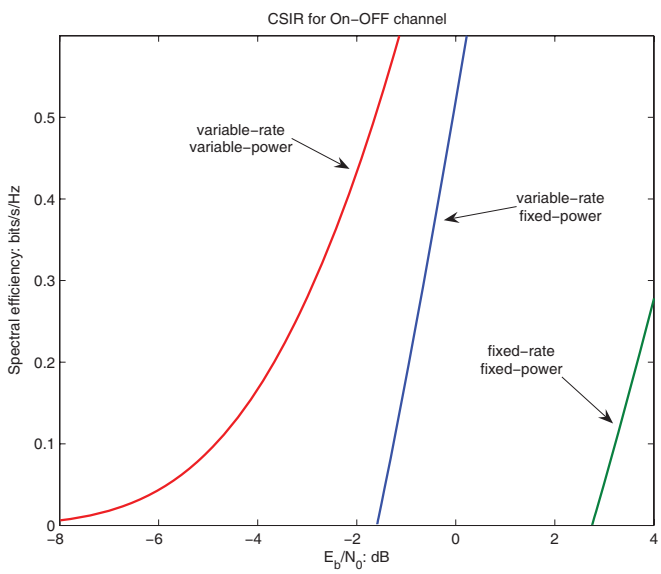

Fig. 8. Spectral efficiency vs. E_b/N_0 in the Rayleigh channel; $\theta = 0.001$.

for fixed-rate/fixed-power transmission schemes considered in this paper.

Remark: From the result of Corollary 1, we note that the analytical and numerical results in this section apply to wideband channels with rich multipath fading. Comparison of Fig. 6 with Fig. 3, where sparse multipath fading scenario is considered, leads to several insightful observations. Note that in both figures, the performance is the same when $\theta = 0$. Hence, in the absence of QoS constraints, multipath sparsity or richness has no effect. This also confirms the claim in the proof of Corollary 2 that low-power and wideband regimes are equivalent when θ. However, we see a stark difference when $\theta > 0$. We observe that multipath sparsity and having the number of subchannels bounded in the wideband regime increases the bit energy requirements significantly especially when θ is large. Moreover, while the minimum bit energy is

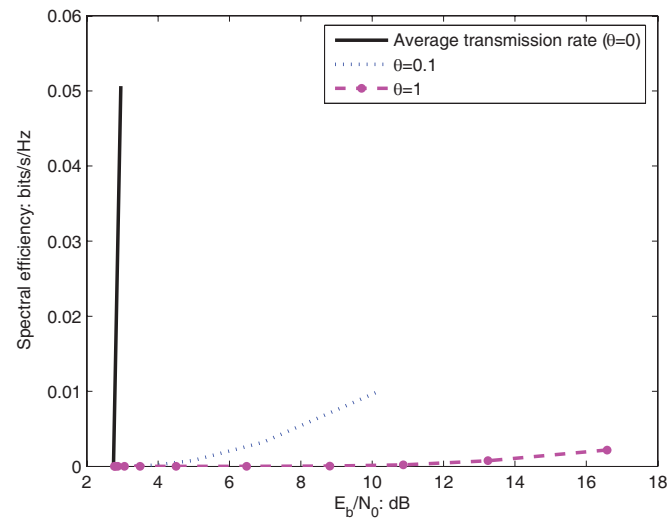

Fig. 9. Spectral efficiency vs. E_b/N_0 in the Rayleigh channel. The number of subchannels N increases sublinearly with bandwidth.

the same for all θ in Fig. 6, the minimum bit energy increases with increasing θ in Fig. 3.

In Section IV, the number of subchannels are assumed to be bounded. In this section, we have considered the rich multipath fading channels in which the number of subchannels increases linearly with bandwidth. A scenario in between these two cases is the one in which the number of subchannels N increases but only sublinearly with increasing bandwidth. As N increases, each subchannel is allocated less power and operate in the low-power regime. At the same time, since N increases sublinearly with B, the coherence bandwidth $B_c = B/N$ also increases. Therefore, the minimum bit energy and wideband slope expressions for this scenario can be obtained by letting B in the results of Theorem 3 go to infinity. Note that under the conditions of Theorem 4, α^*_{opt} is unique and hence does not depend on the bandwidth.

Corollary 3: In the wideband regime, if the number of subchannels N increases sublinearly with B and if fading coefficients in different subchannels are i.i.d. and the probability density function p_z satisfies the conditions in Theorem 4, then the minimum bit energy and wideband slope are given by

$$\frac{E_b}{N_0}_{\min} = \frac{\log_e 2}{\alpha^*_{\text{opt}} P\{z > \alpha^*_{\text{opt}}\}} \quad \text{and} \tag{32}$$

$$\mathcal{S}_0 = \begin{cases} 2P\{z > \alpha^*_{\text{opt}}\} & \theta = 0 \\ 0 & \theta > 0 \end{cases}. \tag{33}$$

In this result, we see that although the same minimum bit energy is attained for all $\theta \geq 0$, approaching this minimum energy level is extremely slow and demanding when $\theta > 0$ due to zero wideband slope. This result is illustrated numerically in Fig. 9.

VI. Conclusion

In this paper, we have considered the effective capacity as a measure of the maximum throughput under statistical QoS constraints, and analyzed the energy efficiency of fixed-rate transmission schemes over fading channels. In particular, we have investigated the spectral efficiency–bit energy tradeoff

in the low-power and wideband regimes. We have obtained expressions for the bit energy at zero spectral efficiency and the wideband slope, which provide a linear approximation to the spectral efficiency curve at low SNRs. In the initial analysis of the wideband regime with bounded number of resolvable paths and hence bounded number of subchannels, we have determined that the bit energy required at zero spectral efficiency (or equivalently at infinite bandwidth) is the minimum bit energy. In this case, we have noted that the minimum bit energy and wideband slope in general depend on the QoS exponent θ. As the QoS constraints become more stringent and hence θ is increased, we have observed in the numerical results that the required minimum bit energy increases. Subsequently, we have considered the low-power regime, which can also be equivalently regarded as the wideband regime with rich multipath fading. We have obtained expressions for the bit energy required at zero spectral efficiency, and wideband slope. For a certain class of fading distributions, we have shown that the bit energy at zero spectral efficiency is indeed the minimum bit energy and is achieved regardless of how strict the QoS constraints are. However, we have also noted that the wideband slope decreases as θ increases, increasing the energy requirements at nonzero spectral efficiency values. Overall, we have quantified the increased energy requirements in the presence of QoS constraints in both wideband and low-power regimes, and identified the impact upon the energy efficiency of multipath sparsity and richness in the wideband regime.

APPENDIX

A. Proof of Theorem 1

In [16, Chap. 7, Example 7.2.7], it is shown for Markov modulated processes that

$$\frac{\Lambda(\theta)}{\theta} = \frac{1}{\theta}\log_e sp\left(\mathbf{\Phi}(\theta)\mathbf{P}\right) \tag{34}$$

where $sp\left(\mathbf{\Phi}(\theta)\mathbf{P}\right)$ is the spectral radius (i.e., the maximum of the absolute values of the eigenvalues) of the matrix $\mathbf{\Phi}(\theta)\mathbf{P}$, $\mathbf{P}$ is the transition matrix of the underlying Markov process, and $\mathbf{\Phi}(\theta)$ is a diagonal matrix whose j^{th} component, $\phi_j(\theta)$, is the moment generating function of the random process $y_j(t)$ given in this state. Hence, we have $\phi_j(\theta) = E\{e^{\theta y_j(t)}\}$.

The transmission model described for the wideband channel with N subchannels is a Markov-modulated process where the underlying Markov process has $N+1$ states with the transition probabilities given in (17). Hence, the transition matrix is given by (35) on the next page. Note that the rows of $\mathbf{P}$ are identical due to the fact that the transition probabilities do not depend on the initial state. In each state, the transmission rate is non-random and fixed. Recall that in state j, the transmission rate is equal to $(j-1)rT$. The moment generating function of this deterministic process is $\phi_j(\theta) = E\{e^{\theta(j-1)rT}\} = e^{\theta(j-1)rT}$. Therefore, we can express $\mathbf{\Phi}(\theta)\mathbf{P}$ as in (36) on the next page.

Note that the rows of $\mathbf{\Phi}(\theta)\mathbf{P}$ are multiples of each other, and hence $\mathbf{\Phi}(\theta)\mathbf{P}$ is a matrix of unit rank. This leads to the conclusion that

$$sp\left(\mathbf{\Phi}(\theta)\mathbf{P}\right) = \text{trace}(\mathbf{\Phi}(\theta)\mathbf{P}) = \sum_{j=1}^{N+1} p_j\, e^{\theta(j-1)rT}. \tag{37}$$

Therefore, for the wideband channel in consideration, we have

$$\frac{\Lambda(\theta)}{\theta} = \frac{1}{\theta}\log_e sp\left(\mathbf{\Phi}(\theta)\mathbf{P}\right) = \frac{1}{\theta}\log_e\left(\sum_{j=1}^{N+1} p_j\, e^{\theta(j-1)rT}\right). \tag{38}$$

Applying the definition

$$\mathsf{R}_E(\text{SNR},\theta) = \frac{1}{TB}\max_{\substack{r\geq 0\\ \bar{P}_k\geq 0 \text{ s.t. } \sum \bar{P}_k\leq \bar{P}}}\left\{-\frac{\Lambda(-\theta)}{\theta}\right\} \tag{39}$$

where we have maximization over the transmission rates and power allocation strategies, we immediately obtain (19).

Assume now that $\{z_k\}_{k=1}^N$ are identically distributed and therefore p_j is in the binomial form given in (18). Then, we can easily obtain (40)–(43) on the next page. Note that (41) is obtained by applying a change of variables with $i = j-1$ and combining the second and fourth terms in the summation in (40) to write $\left(P\{z>\alpha\}e^{\theta rT}\right)^i$. (42) follows from the Binomial Theorem. Now, the expression in (20) is readily obtained by noting that $\frac{B}{N} = B_c$. □

B. Proof of Theorem 2

Assume that the Taylor series expansion of r_{opt} with respect to small $\zeta = \frac{1}{B_c}$ is

$$r_{\text{opt}} = r^*_{\text{opt}} + \dot{r}_{\text{opt}}(0)\zeta + o(\zeta) \tag{44}$$

where $r^*_{\text{opt}} = \lim_{\zeta\to 0} r_{\text{opt}}$ and $\dot{r}_{\text{opt}}(0)$ is the first derivative with respect to ζ of r_{opt} evaluated at $\zeta = 0$. From (4), we can find that

$$\begin{aligned}\alpha_{\text{opt}} &= \frac{2^{r_{\text{opt}}\zeta}-1}{\frac{\bar{P}\zeta}{NN_0}}\\ &= \frac{r^*_{\text{opt}}\log_e 2}{\frac{\bar{P}}{NN_0}} + \frac{\dot{r}_{\text{opt}}(0)\log_e 2 + \frac{(r^*_{\text{opt}}\log_e 2)^2}{2}}{\frac{\bar{P}}{NN_0}}\zeta + o(\zeta)\end{aligned} \tag{45}$$

from which we have as $\zeta\to 0$ that

$$\alpha^*_{\text{opt}} = \frac{r^*_{\text{opt}}\log_e 2}{\frac{\bar{P}}{NN_0}} \quad \text{and} \tag{46}$$

$$\dot{\alpha}_{\text{opt}}(0) = \frac{\dot{r}_{\text{opt}}(0)\log_e 2 + \frac{(r^*_{\text{opt}}\log_e 2)^2}{2}}{\frac{\bar{P}}{NN_0}} \tag{47}$$

where $\dot{\alpha}_{\text{opt}}(0)$ is the first derivative with respect to ζ of α_{opt} evaluated at $\zeta = 0$. According to (46), $r^*_{\text{opt}} = \frac{\bar{P}\alpha^*_{\text{opt}}}{NN_0\log_e 2}$. We can now derive (48) on the next page where $\dot{\mathsf{R}}_E(0)$ is the derivative of R_E with respect to ζ at $\zeta = 0$,

$$\delta = \frac{\theta T\bar{P}}{NN_0\log_e 2},$$

and

$$\xi = 1 - P\{z>\alpha^*_{\text{opt}}\}(1-e^{-\delta\alpha^*_{\text{opt}}}).$$

$$\mathbf{P} = \begin{bmatrix} p_{1,1} & p_{1,2} & \cdot & \cdot & p_{1,N+1} \\ \cdot & & & & \cdot \\ \cdot & & & & \cdot \\ p_{N+1,1} & p_{N+1,2} & \cdot & \cdot & p_{N+1,N+1} \end{bmatrix} = \begin{bmatrix} p_1 & p_2 & \cdot & \cdot & p_{N+1} \\ \cdot & & & & \cdot \\ \cdot & & & & \cdot \\ p_1 & p_2 & \cdot & \cdot & p_{N+1} \end{bmatrix}. \tag{35}$$

$$\mathbf{\Phi}(\theta)\mathbf{P} = \underbrace{\begin{bmatrix} 1 & 0 & . & . & 0 \\ 0 & e^{\theta rT} & 0 & . & 0 \\ . & & & & . \\ 0 & 0 & . & 0 & e^{\theta NrT} \end{bmatrix}}_{\mathbf{\Phi}(\theta)} \underbrace{\begin{bmatrix} p_1 & p_2 & \cdot & \cdot & p_{N+1} \\ \cdot & & & & \cdot \\ \cdot & & & & \cdot \\ p_1 & p_2 & \cdot & \cdot & p_{N+1} \end{bmatrix}}_{\mathbf{P}} = \begin{bmatrix} p_1 & p_2 & \cdot & \cdot & p_{N+1} \\ p_1 e^{\theta rT} & p_2 e^{\theta rT} & \cdot & \cdot & p_{N+1} e^{\theta rT} \\ \cdot & & & & \cdot \\ p_1 e^{\theta NrT} & p_2 e^{\theta NrT} & \cdot & \cdot & p_{N+1} e^{\theta NrT} \end{bmatrix}. \tag{36}$$

$$\sum_{j=1}^{N+1} p_j\, e^{\theta(j-1)rT} = \sum_{j=1}^{N+1} \binom{N}{j-1} (P\{z>\alpha\})^{j-1} (1-P\{z>\alpha\})^{N-j+1}\, e^{\theta(j-1)rT} \tag{40}$$

$$= \sum_{i=0}^{N} \binom{N}{i} \left(P\{z>\alpha\} e^{\theta rT}\right)^{i} (1-P\{z>\alpha\})^{N-i} \tag{41}$$

$$= (1-P\{z>\alpha\} + P\{z>\alpha\} e^{\theta rT})^N \tag{42}$$

$$= (1-P\{z>\alpha\}(1-e^{\theta rT}))^N. \tag{43}$$

$$\left.\frac{E_b}{N_0}\right|_{\mathsf{R}_E=0} = \lim_{\zeta\to 0} \frac{\frac{\bar{P}}{NN_0}\zeta}{\mathsf{R}_E(\zeta)} = \frac{\frac{\bar{P}}{NN_0}}{\dot{\mathsf{R}}_E(0)} = \frac{-\frac{\theta T\bar{P}}{NN_0}}{\log_e\left(1-P\{z>\alpha^*_{\text{opt}}\}(1-e^{-\theta T r^*_{\text{opt}}})\right)} = \frac{-\delta \log_e 2}{\log_e \xi} \tag{48}$$

Since $\frac{E_b}{N_0} = \frac{\frac{\bar{P}}{NN_0}}{\frac{\mathsf{R}_E(\zeta)}{\zeta}}$, the result that $\left.\frac{E_b}{N_0}\right|_{\mathsf{R}_E=0} = \frac{E_b}{N_0}\min$ follows from the fact that $\mathsf{R}_E(\zeta)/\zeta$ monotonically decreases with increasing ζ, and hence achieves its maximum as $\zeta \to 0$. Therefore, we prove (22).

The second derivative $\ddot{\mathsf{R}}_E(0)$, required in the computation of the wideband slope $\mathcal{S}_0$, is derived through (49)–(52) on the next page where $r^*_{\text{opt}} = \frac{\bar{P}\alpha^*_{\text{opt}}}{NN_0 \log_e 2}$. Note that (51) and (52) follow by using L'Hospital's Rule and applying Leibniz Integral Rule [24].

Next, we derive an equality satisfied by α^*_{opt}. Consider the objective function in (20)

$$-\frac{1}{\theta T B_c} \log_e\left(1-P\{z>\alpha\}(1-e^{-\theta T r})\right). \tag{53}$$

It can easily be seen that both as $r \to 0$ and $r \to \infty$, this objective function approaches zero[5]. Hence, (53) is maximized at a finite and nonzero value of r at which the derivative of (53) with respect to r is zero. Differentiating (53) with respect to r and making it equal to zero leads to the following equality that needs to be satisfied at the optimal value r_{opt}:

$$\frac{2^{r_{\text{opt}}\zeta} p_z(\alpha_{\text{opt}}) NN_0 \log_e 2}{\bar{P}}(1-e^{-\theta T r_{\text{opt}}}) = \theta T e^{-\theta T r_{\text{opt}}} P\{z>\alpha_{\text{opt}}\} \tag{54}$$

where $\zeta = 1/B_c$. For given θ, as the bandwidth increases (i.e., $\zeta \to 0$), $r_{\text{opt}} \to r^*_{\text{opt}}$. Clearly, $r^*_{\text{opt}} \neq 0$ in the wideband regime. Because, otherwise, if $r_{\text{opt}} \to 0$ and consequently $\alpha_{\text{opt}} \to 0$, the left-hand-side of (54) becomes zero, while the right-hand-side is different from zero. So, employing (46) and taking the limit of both sides of (54) as $\zeta \to 0$, we can derive

$$\frac{p_z(\alpha^*_{\text{opt}}) NN_0 \log_e 2}{\bar{P}}\left(1-e^{-\frac{\theta T\bar{P}}{NN_0\log_e 2}\alpha^*_{\text{opt}}}\right) = \theta T e^{-\frac{\theta T\bar{P}}{NN_0\log_e 2}\alpha^*_{\text{opt}}} P\{z>\alpha^*_{\text{opt}}\} \tag{55}$$

which, after rearranging, yields

$$\frac{\theta T\bar{P}}{NN_0\log_e 2}\alpha^*_{\text{opt}} = \log_e\left(1+\frac{\theta T\bar{P}}{NN_0\log_e 2}\frac{P\{z>\alpha^*_{\text{opt}}\}}{p_z(\alpha^*_{\text{opt}})}\right). \tag{56}$$

Denoting $\delta = \frac{\theta T\bar{P}}{NN_0\log_e 2}$, we obtain the condition (24) stated in the theorem.

Combining (55) and (47) with (52) gives us

$$\ddot{\mathsf{R}}_E(0) = -\frac{NN_0\log_e^2 2}{\theta T\bar{P}} \frac{{r^*_{\text{opt}}}^2 p_z(\alpha^*_{\text{opt}})(1-e^{-\theta T r^*_{\text{opt}}})}{1-P\{z>\alpha^*_{\text{opt}}\}\left(1-e^{-\theta T r^*_{\text{opt}}}\right)} = -\frac{{r^*_{\text{opt}}}^2 P\{z>\alpha^*_{\text{opt}}\} e^{-\theta T r^*_{\text{opt}}}\log_e 2}{1-P\{z>\alpha^*_{\text{opt}}\}\left(1-e^{-\theta T r^*_{\text{opt}}}\right)} \tag{57}$$

Substituting (57) and the expression for $\dot{\mathsf{R}}_E(0)$ in (48) into (14), we obtain (23). □

C. Proof of Theorem 3

We first consider the Taylor series expansion of r_{opt} in the low-SNR regime:

$$r_{\text{opt}} = a\text{SNR} + b\text{SNR}^2 + o(\text{SNR}^2) \tag{58}$$

[5]Note that α increases without bound with increasing r.

$$\ddot{\mathsf{R}}_E(0) = \lim_{\zeta\to 0} 2\frac{\mathsf{R}_E(\zeta) - \dot{\mathsf{R}}_E(0)\zeta}{\zeta^2} \tag{49}$$

$$= \lim_{\zeta\to 0} 2\frac{1}{\zeta}\Big(-\frac{1}{\theta T}\log_e\big(1 - P\{z > \alpha_{\text{opt}}\}\big(1 - e^{-\theta T r_{\text{opt}}}\big)\big) + \frac{1}{\theta T}\log_e\big(1 - P\{z > \alpha^*_{\text{opt}}\}(1 - e^{-\theta T r^*_{\text{opt}}})\big)\Big) \tag{50}$$

$$= \lim_{\zeta\to 0} -\frac{2}{\theta T}\frac{\big(p_z(\alpha_{\text{opt}})\dot{\alpha}_{\text{opt}}(\zeta)(1 - e^{-\theta T r_{\text{opt}}}) - P\{z > \alpha_{\text{opt}}\}\theta T e^{-\theta T r_{\text{opt}}}\dot{r}_{\text{opt}}(\zeta)\big)}{1 - P\{z > \alpha_{\text{opt}}\}\big(1 - e^{-\theta T r_{\text{opt}}}\big)} \tag{51}$$

$$= -\frac{2}{\theta T}\frac{\big(p_z(\alpha^*_{\text{opt}})\dot{\alpha}_{\text{opt}}(0)(1 - e^{-\theta T r^*_{\text{opt}}}) - P\{z > \alpha^*_{\text{opt}}\}\theta T e^{-\theta T r^*_{\text{opt}}}\dot{r}_{\text{opt}}(0)\big)}{1 - P\{z > \alpha^*_{\text{opt}}\}\big(1 - e^{-\theta T r^*_{\text{opt}}}\big)} \tag{52}$$

where a and b are real-valued constants. Substituting (58) into (4), we obtain the Taylor series expansion for α_{opt}:

$$\alpha_{\text{opt}} = \frac{a\log_e 2}{B} + \left(\frac{b\log_e 2}{B} + \frac{a^2\log_e^2 2}{2B^2}\right)\text{SNR} + o(\text{SNR}). \tag{59}$$

From (59), we note that in the limit as $\text{SNR} \to 0$, we have

$$\alpha^*_{\text{opt}} = \frac{a\log_e 2}{B}. \tag{60}$$

Next, we obtain the Taylor series expansion with respect to SNR for $P\{z > \alpha_{\text{opt}}\}$ using the Leibniz Integral Rule [24] as in (61) on the next page.

Using (58), (59), and (61), we find the series expansion for R_E given in (12) as in (62) on the next page. Then, using (60), we immediately derive from (62) that

$$\dot{\mathsf{R}}_E(0) = \frac{\alpha^*_{\text{opt}}P\{z > \alpha^*_{\text{opt}}\}}{\log_e 2}, \tag{63}$$

$$\ddot{\mathsf{R}}_E(0) = -\frac{{\alpha^*_{\text{opt}}}^3 p_z\{\alpha^*_{\text{opt}}\}}{\log_e 2} - \frac{\theta T B {\alpha^*_{\text{opt}}}^2}{\log_e^2 2}P\{z > \alpha^*_{\text{opt}}\}(1 - P\{z > \alpha^*_{\text{opt}}\}). \tag{64}$$

Similarly as in the discussion in the proof of Theorem 2 in Section IV, the optimal fixed-rate r_{opt}, akin to (54), should satisfy

$$\frac{2^{r_{\text{opt}}/B}p_z(\alpha_{\text{opt}})\log_e 2}{B\text{SNR}}(1 - e^{-\theta T r_{\text{opt}}}) = \theta T e^{-\theta T r_{\text{opt}}}P\{z > \alpha_{\text{opt}}\}. \tag{65}$$

Taking the limits of both sides of (65) as $\text{SNR} \to 0$ and employing (58), we obtain

$$\frac{a p_z(\alpha^*_{\text{opt}})\log_e 2}{B} = P\{z > \alpha^*_{\text{opt}}\}. \tag{66}$$

From (60), (66) simplifies to

$$\alpha^*_{\text{opt}}p_z(\alpha^*_{\text{opt}}) = P\{z > \alpha^*_{\text{opt}}\}, \tag{67}$$

proving the condition in (28). Moreover, using (67), the first term in the expression for $\ddot{\mathsf{R}}_E(0)$ in (64) becomes $-\frac{{\alpha^*_{\text{opt}}}^2 P\{z \geq \alpha^*_{\text{opt}}\}}{\log_e 2}$. Together with this change, evaluating the expressions in (14) with the results in (63) and (64), we obtain (26) and (27). □

REFERENCES

[1] S. Verdú, "Spectral efficiency in the wideband regime," *IEEE Trans. Inform. Theory*, vol. 48, no. 6 pp. 1319-1343. June 2002.

[2] A. Ephremides and B. Hajek, "Information theory and communication networks: an unconsummated union," *IEEE Trans. Inform. Theory*, vol. 44, pp. 2416-2434, Oct. 1998.

[3] S. V. Hanly and D. N. C. Tse, "Multiaccess fading channels–part II: delay-limited capacities," *IEEE Trans. Inform. Theory*, vol. 44, no. 7, pp. 2816-2831. Nov. 1998.

[4] D. Wu and R. Negi, "Effective capacity: a wireless link model for support of quality of service," *IEEE Trans. Wireless Commun.*, vol. 2, no. 4, pp. 630-643, July 2003

[5] D. Wu and R. Negi, "Downlink scheduling in a cellular network for quality-of-service assurance," *IEEE Trans. Veh. Technol.*, vol. 53, no. 5, pp. 1547-1557, Sept. 2004.

[6] D. Wu and R. Negi, "Utilizing multiuser diversity for efficient support of quality of service over a fading channel, *IEEE Trans. Veh. Technol.*, vol. 49, pp. 1073-1096, May 2003.

[7] J. Tang and X. Zhang, "Quality-of-service driven power and rate adaptation over wireless links, *IEEE Trans. Wireless Commun.*, vol. 6, no. 8, pp. 3058-3068, Aug. 2007.

[8] J. Tang and X. Zhang, "Quality-of-service driven power and rate adaptation for multichannel communications over wireless links, *IEEE Trans. Wireless Commun.*, vol. 6, no. 12, pp. 4349-4360, Dec. 2007.

[9] J. Tang and X. Zhang, "Cross-layer modeling for quality of service guarantees over wireless links, *IEEE Trans. Wireless Commun.*, vol. 6, no. 12, pp. 4504-4512, Dec. 2007.

[10] J. Tang and X. Zhang, "Cross-layer-model based adaptive resource allocation for statistical QoS guarantees in mobile wireless networks, *IEEE Trans. Wireless Commun.*, vol. 7, pp. 2318-2328, June 2008.

[11] L. Liu, P. Parag, J. Tang, W.-Y. Chen, and J.-F. Chamberland, "Resource allocation and quality of service evaluation for wireless communication systems using fluid models," *IEEE Trans. Inform. Theory*, vol. 53, no. 5, pp. 1767-1777, May 2007

[12] L. Liu, P. Parag, and J.-F. Chamberland, "Quality of service analysis for wireless user-cooperation networks," *IEEE Trans. Inform. Theory*, vol. 53, no. 10, pp. 3833-3842, Oct. 2007

[13] L. Liu and J.-F. Chamberland, "On the effective capacities of multiple-antenna Gaussian channels," IEEE International Symposium on Information Theory, Toronto, 2008.

[14] M. C. Gursoy, D. Qiao, and S. Velipasalar, "Analysis of energy efficiency in fading channel under QoS constraints," *IEEE Trans. Wireless Commun.*, vol. 8, no. 8, pp. 4252–4263, Aug. 2009.

[15] C.-S. Chang, "Stability, queue length, and delay of deterministic and stochastic queuing networks," *IEEE Trans. Auto. Control*, vol. 39, no. 5, pp. 913-931, May 1994

[16] C.-S. Chang, *Performance Guarantees in Communication Networks*. New York: Springer, 1995

[17] C.-S. Chang and T. Zajic, "Effective bandwidths of departure processes from queues with time varying capacities," in *Proc. IEEE Infocom,* pp. 1001-1009, 1995

[18] P. Sadeghi and P. Rapajic, "Capacity analysis for finite-state Markov mapping of flat-fading channels," *IEEE Trans. Commun.*, vol. 53, pp. 833-840, May 2005.

[19] D. Porrat, D. N. C. Tse, and S. Nacu, "Channel uncertainty in ultra-wideband communication systems," *IEEE Trans. Inform. Theory*, vol. 53, pp. 194-208, Jan. 2007.

[20] V. Raghavan, G. Hariharan, and A. M. Sayeed, "Capacity of sparse multipath channels in the ultra-wideband regime," *IEEE J. Select. Topics Signal Processing*, vol. 1, pp. 357-371, Oct. 2007.

[21] E. Telatar and D. N. C. Tse, "Capacity and mutual information of wideband multipath fading channels," *IEEE Trans. Inform. Theory*, vol. 46, pp. 1384-1400, July 2000.

[22] A. Goldsmith, *Wireless Communications*, 1st ed. Cambridge University Press, 2005.

$$P\{z > \alpha_{\text{opt}}\} = P\{z > \alpha^*_{\text{opt}}\} - \left(\frac{b\log_e 2}{B} + \frac{a^2\log_e^2 2}{2B^2}\right) p_z(\alpha^*_{\text{opt}})\text{SNR} + o(\text{SNR}). \tag{61}$$

$$\begin{aligned}\mathsf{R}_E(\text{SNR}) &= -\frac{1}{\theta TB}\log_e\Bigg[1 - \left(P\{z > \alpha^*_{\text{opt}}\} - \left(\frac{b\log_e 2}{B} + \frac{a^2\log_e^2 2}{2B^2}\right)p_z(\alpha^*_{\text{opt}})\text{SNR} + o(\text{SNR})\right) \\ &\qquad \times \left(\theta Ta\text{SNR} + (\theta Tb - \frac{(\theta Ta)^2}{2})\text{SNR}^2 + o(\text{SNR}^2)\right)\Bigg] \\ &= \frac{aP\{z > \alpha^*_{\text{opt}}\}}{B}\text{SNR} + \frac{1}{B}\Big(-\frac{\theta Ta^2}{2}P\{z > \alpha^*_{\text{opt}}\} - \frac{a^3 p_z(\alpha^*_{\text{opt}})\log_e^2 2}{2B^2} + \frac{\theta T(P\{z > \alpha^*_{\text{opt}}\}a)^2}{2}\Big)\text{SNR}^2 + o(\text{SNR}^2).\end{aligned} \tag{62}$$

[23] T. Szigeti and C. Hattingh, *End-to-End QoS Network Design: Quality of Service in LANs, WANs, and VPNs*. Cisco Press, 2004.

[24] M. H. Protter, C. B. Morrey, and C. B. Morrey, Jr., *A First Course in Real Analysis*, 2nd ed. Springer, 1991.

[25] G. R. Grimmett and D. R. Stirzaker, *Probability and Random Processes*, 2nd ed. Oxford University Press, 1998.

[26] I. S. Gradshteyn and I. M. Ryzhik, *Table of Integrals, Series, and Products*. Academic Press, 2000.

Deli Qiao received the B.E. degree in electrical engineering from Harbin Institute of Technology, Harbin, China, in 2007. He is currently a research assistant working towards the Ph.D. degree in the Department of Electrical Engineering, University of Nebraska-Lincoln, Lincoln, NE, US. His research interests include information theory and wireless communications, with an emphasis on quality of service (QoS) provisioning.

Mustafa Cenk Gursoy received the B.S. degree in electrical and electronic engineering from Bogazici University, Istanbul, Turkey, in 1999, and the Ph.D. degree in electrical engineering from Princeton University, Princeton, NJ, USA, in 2004. He was a recipient of the Gordon Wu Graduate Fellowship from Princeton University between 1999 and 2003. In the summer of 2000, he worked at Lucent Technologies, Holmdel, NJ, where he conducted performance analysis of DSL modems. Since September 2004, he has been an Assistant Professor in the Department of Electrical Engineering at the University of Nebraska-Lincoln (UNL). His research interests are in the general areas of wireless communications, information theory, communication networks, and signal processing. He received an NSF CAREER Award in 2006, UNL College Distinguished Teaching Award in 2009, and the 2004-2007 EURASIP JOURNAL OF WIRELESS COMMUNICATIONS AND NETWORKING Best Paper Award.

Senem Velipasalar is currently an assistant professor in the Department of Electrical Engineering at the University of Nebraska-Lincoln (UNL). She received the Ph.D. and M.A. degrees in Electrical Engineering from Princeton University in 2007 and 2004, respectively, the M.S. degree in Electrical Sciences and Computer Engineering from Brown University in 2001, and the B.S. degree in Electrical and Electronic Engineering with high honors from Bogazici University, Turkey in 1999. Her research interests include computer vision, video/image processing, distributed smart camera systems, pattern recognition, statistical learning, and signal processing. During the summers of 2001 through 2005, she worked in the Exploratory Computer Vision Group at IBM T.J. Watson Research Center. She is the recipient of IBM Patent Application Award, and Princeton and Brown University Graduate Fellowships. She received the Best Student Paper Award at the IEEE International Conference on Multimedia & Expo (ICME) in 2006. She is a member of the IEEE.